AIP | Applied Physics Letters

Detecting optically synthesized quasi-monochromatic sub-terahertz phonon wavepackets by ultrafast x-ray diffraction

M. Herzog, A. Bojahr, J. Goldshteyn, W. Leitenberger, I. Vrejoiu et al.

Citation: Appl. Phys. Lett. **100**, 094101 (2012); doi: 10.1063/1.3688492
View online: http://dx.doi.org/10.1063/1.3688492
View Table of Contents: http://apl.aip.org/resource/1/APPLAB/v100/i9
Published by the American Institute of Physics.

Detecting optically synthesized quasi-monochromatic sub-terahertz phonon wavepackets by ultrafast x-ray diffraction

M. Herzog,[1] A. Bojahr,[1] J. Goldshteyn,[2] W. Leitenberger,[1] I. Vrejoiu,[3] D. Khakhulin,[4] M. Wulff,[4] R. Shayduk,[2] P. Gaal,[1] and M. Bargheer[1,2,a)]

[1]*Institut für Physik und Astronomie, Universität Potsdam, Karl-Liebknecht-Str. 24-25, 14476 Potsdam, Germany*

[2]*Helmholtz-Zentrum Berlin für Materialien und Energie GmbH, Wilhelm-Conrad-Röntgen Campus, BESSY II, Albert-Einstein-Str. 15, 12489 Berlin, Germany*

[3]*Max-Planck-Institut für Mikrostrukturphysik, Weinberg 2, 06120 Halle, Germany*

[4]*European Synchrotron Radiation Facility (ESRF), 6 rue Jules Horowitz, 38000 Grenoble, France*

(Received 10 January 2012; accepted 7 February 2012; published online 27 February 2012)

We excite an epitaxial $SrRuO_3$ thin film transducer by a pulse train of ultrashort laser pulses, launching coherent sound waves into the underlying $SrTiO_3$ substrate. Synchrotron-based x-ray diffraction (XRD) data exhibiting separated sidebands to the substrate peak evidence the excitation of a quasi-monochromatic phonon wavepacket with sub-THz central frequency. The frequency and bandwidth of this sound pulse can be controlled by the optical pulse train. We compare the experimental data to combined lattice dynamics and dynamical XRD simulations to verify the coherent phonon dynamics. In addition, we observe a lifetime of 130 ps of such sub-THz phonons in accordance with the theory. © *2012 American Institute of Physics*. [http://dx.doi.org/10.1063/1.3688492]

Ultrafast x-ray diffraction (UXRD) is a powerful tool for monitoring atomic motion in solids on the related length and timescales. In principle, each displacement field within a crystal can be decomposed into discrete phonon modes of respective frequency ω and wavevector Q which are related by the phonon dispersion relation $\omega = \omega(Q)$. One key aspect of UXRD is the direct correspondence of a phonon-induced real-space periodicity $\lambda = 2\pi/Q$ within a host crystal of lattice spacing c and the finite diffraction intensity at wavevector transfer $q = |\mathbf{k}_{in} - \mathbf{k}_{out}| = G \pm Q$, where $\mathbf{k}_{in}$ and $\mathbf{k}_{out}$ are the incident and diffracted x-ray photon wavevectors, respectively, and $G = 2\pi/c$ is the reciprocal lattice vector of the host crystal.[1,2] This relation is depicted in Fig. 1(a) for $G + Q$. Each phonon mode Q is, thus, responsible for x-rays diffracted into sharp sidebands of the main crystal Bragg reflection at $G \pm Q$ which oscillate at their respective eigenfrequency $\omega(Q)$. These features have been theoretically discussed by Larsson *et al.*[2]

Early UXRD experiments verified these relations by observing UXRD signals of longitudinal acoustic (LA) phonons in bulk crystals.[1–3] In these experiments, the intense and ultrashort laser pulses excite bipolar strain waves into the bulk crystal[4] which have a broad phonon spectrum that accordingly generates contributions in a broad vicinity of the bulk Bragg reflection. The linear dispersion relation of LA phonons, $\omega = v_{LA}Q$, was verified by tuning q, where v_{LA} is the LA sound velocity.

For various physical and technical issues (such as phonon spectroscopy, phonon-phonon scattering, etc.), it is favorable to selectively generate high-frequency monochromatic phonon beams instead of spectrally broad pulses as in the first UXRD experiments. Several techniques have been developed, e.g., via thermomodulation[5] or piezoelectric transducers.[6] Roshchupkin and co-workers observed XRD sidebands due to continuous surface acoustic waves in langatate crystals.[7] Acoustoelectrically amplified phonons below 10 GHz forming a continuous monochromatic bulk sound wave have also been detected by XRD.[6] Solely optical techniques provide tunability of the phonon frequencies into the THz region. Optical multi-pulse excitation has been used to coherently control LA phonons in bulk InSb.[8] Recently, high-frequency narrow-bandwidth tunable LA phonon pulses were coherently excited by optical pulse trains and subsequently verified by optical means.[9,10] Alternatively, the single-pulse photoexcitation of semiconductor superlattices generates folded LA phonons.[11,12] Due to coupling to the substrate, these folded phonons unfold into the substrate which results in similar phonon pulses as discussed here.[13] Such unfolding could be monitored by UXRD; however, the corresponding weak signatures in the diffraction curves were mainly dominated by the strong superlattice Bragg peaks.[14] Moreover,

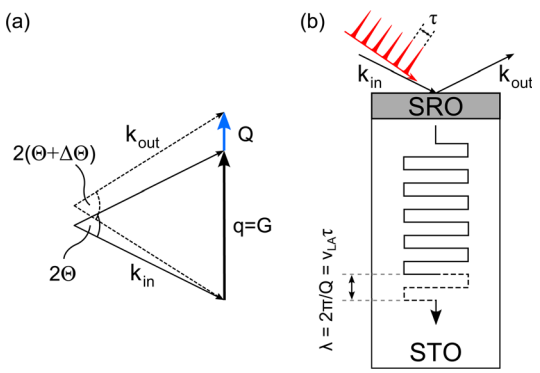

FIG. 1. (Color online) (a) Schematic representation of coherent XRD from a reciprocal lattice vector G (solid lines) and from an additional phonon of wavevector Q (dashed lines). The same process is possible for G and Q being antiparallel. (b) Schematic of the experiment. Each laser pulse launches a bipolar strain wave into the substrate (dashed line) resulting in a phonon wavepacket with central wavevector Q (dashed and solid line).

a)Electronic mail: bargheer@uni-potsdam.de.

these unfolded phonon wavepackets have a fixed central frequency defined by the spatial superlattice period.[13,14]

In this letter, we synthesized a quasi-monochromatic phonon pulse by excitation of a $SrRuO_3$ (SRO) thin film transducer epitaxially grown by pulsed laser deposition[32] on a $SrTiO_3$ substrate[15] with a train of ultrashort optical laser pulses (schematically shown in Fig. 1(b)). Relevant material properties of SRO and STO can be found in, e.g., Refs. 27, 28, 33, and 34. Each laser pulse impulsively launches a single spectrally broad bipolar strain pulse with high amplitude into the substrate (schematically depicted by the dashed line in Fig. 1(b)).[16] The optical pulse train with pulse frequency $\nu = \tau^{-1}$ and N pulses thus synthesizes a coherent phonon wavepacket[10] with wavevector $Q_p = 2\pi\nu/v_{LA}$, where v_{LA} is the LA sound velocity of the STO substrate. Using UXRD, we observe clear sidebands to the STO Bragg peak as the x-ray photons scatter from the monochromatic phonons according to $q = G + Q_p$. The selective excitation of coherent phonons with a specific Q_p allows us to directly monitor the 130 ps lifetime of these sub-THz phonons which undergo strong damping attributed to thermoelastic damping and Akhiezer's mechanism of relaxation damping.[17–19] The central wavevector of the observed wavepacket can be controlled by the pulse repetition rate ν and the bandwidth is inversely proportional to N. By tuning ν, one can thus map out the LA phonon dispersion relation $\omega(Q)$.

The time-resolved XRD experiments were performed at the undulator beamline ID09B at the synchrotron source ESRF.[20] The general experimental setup working at 1 kHz repetition rate was described in Ref. 21. The storage ring was running in 16-bunch mode generating ≈ 100 ps x-ray pulses. We chose a photon energy of 12 keV for the experiments and utilized only one sample (cf. Ref. 21). The optical pulse train was produced by a mirror composed of four alternatingly stacked glass plates and spacer rings giving eight reflections from the air-glass interfaces. The plates and rings had a thickness of 710 μm and 1100 μm, respectively, corresponding to pulse spacing of $\tau \approx 7.2$ ps ($\nu \approx 140$ GHz) at normal incidence, which was verified by optical cross-correlation measurements. Due to the rather low reflectivity of the air-glass interfaces, the energy distribution within the pulse train was almost homogeneous. The integrated fluence at the sample was set to ≈ 44 mJ/cm^2, i.e., each pulse contributed a mean fluence of ≈ 5.5 mJ/cm^2.

The inset of Fig. 2(a) shows the static rocking curve around the (002) STO substrate Bragg peak from which we deduced a SRO layer thickness of ≈ 15.4 nm. The high-angle side of the STO substrate Bragg peak has very little contribution from the SRO layer which allows to observe the sidebands of the phonon wavepackets without any congestion from the top layer(s). This situation is even improved by the shift of the SRO peak towards lower angles due to the photoinduced thermal expansion. The robust perovskite oxide SRO has a fast electron-phonon coupling and is, thus, perfectly suited as a thin film transducer which can be triggered by strong laser-pulse excitation in order to generate phonon spectra with a high frequency cutoff.[22–25]

Figure 2(a) shows the measured rocking curves in the vicinity of the (002) STO substrate Bragg peak before (open black diamonds) and 130 ps after (solid red bullets) the arrival of the first pump pulse of the pulse train. The rocking curve at positive time delay shows a distinct sideband evidencing the excitation of a coherent narrow-bandwidth phonon wavepacket with a central wavevector around $\Delta q = Q_p^{(1)} = 0.11$ nm^{-1}. Moreover, the excitation of the second harmonic around $\Delta q = Q_p^{(2)} = 0.22$ nm^{-1} with much weaker amplitude can be inferred from Fig. 2. Although we observe clearly separated harmonics, the sidebands are rather broad and exhibit additional modulations. The comparatively large penetration depth of the 800 nm pump light in SRO ($\xi_{SRO} \approx 52$ nm) results in nearly homogeneous excitation of the thin film transducer.[13,26] The individual bipolar strain pulses thus roughly have a rectangular and steplike shape and consequently higher harmonics of Q_p are generated. Since we have an independent measure of ν, the linear LA phonon dispersion relation readily yields $v_{LA} \approx 7.9$ nm/ps which perfectly agrees with the literature values.[27,28]

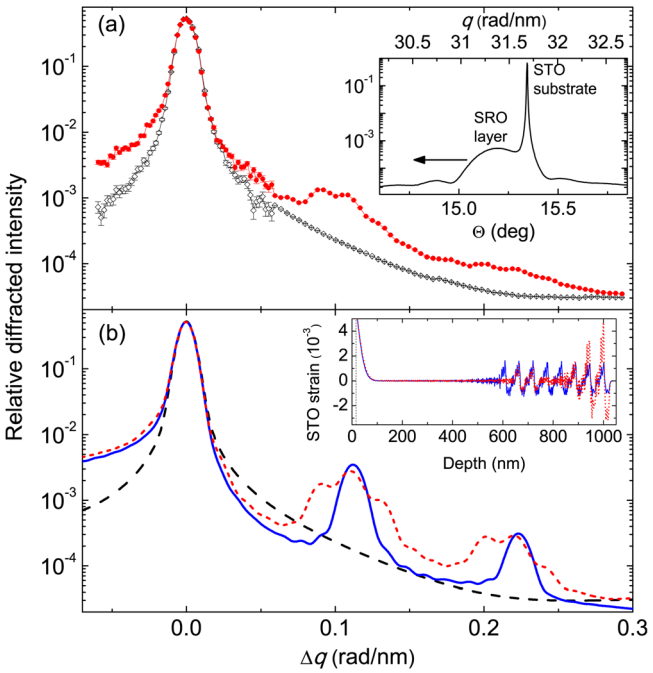

FIG. 2. (Color online) (a) Experimental rocking curves (measured piecewise) of the high-angle side of the STO substrate peak before (open black diamonds) and 130 ps after (solid red bullets) excitation by a pulse train with 7.2 ps pulse separation. Inset: static rocking curve measured with a high-resolution x-ray photodiode. The arrow indicates the shift of the SRO peak due to the photoinduced thermal expansion. (b) Simulations of the measured rocking curves without excitation (long-dashed black) and with excitation by a pulse train having a uniform (solid blue) and non-uniform (short-dashed red) pulse energy distribution. Inset: calculated strain pattern 130 ps after excitation with uniform (solid blue) and non-uniform (dashed red) pulse energy distribution.

In order to understand the experimental data in more detail, we utilized numerical model calculations to simulate the experiment. First, we use a linear-chain model of masses and springs to calculate the coherent lattice dynamics.[13] The multiple pump pulse excitation necessitates the inclusion of heat diffusion into the simulation. The resulting spatio-temporal strain maps then serve as an input for dynamical XRD simulations to calculate the transient rocking curves.[26,29] The simulated transient rocking curves are plotted in Fig. 2(b). We first assume a pulse train of 8 identical pulses with 7.2 ps pulse separation. The calculated strain field at 130 ps is shown in the inset of Fig. 2(b). The corresponding rocking

curve (solid blue) exhibits sharp Bragg peaks at the experimentally observed wavevector $\Delta q = 0.11\ \mathrm{nm}^{-1}$ and its higher harmonics.

The experimental peak width is much broader than for the idealized simulation. This may originate from varying pulse energies at the probe area. For instance, a different pointing of the individual optical pump beams due to non-parallel glass plates of the mirror stack would generate different excitation densities at the fairly distant probe spot for each pulse. To account for such effects, we further assumed a non-uniform pump pulse energy distribution within the pulse train which results in the dashed red curve in Fig. 2. This rocking curve satisfactorily approximates the shape of the experimental data. The individual pulse energies are proportional to the corresponding amplitudes of the bipolar strain pulses plotted in the inset of Fig. 2(b). Thus, a controlled variation of the pulse energy distribution in principle allows to generate arbitrary phonon spectra in addition to the tunability of the central wavevector by the pulse frequency ν.

Finally, we analyze the time-dependence of the first-order sideband of the phonon wavepacket. For this, we evaluate the integrated intensity of the main part between $\Delta q = 0.08$ rad/nm and $\Delta q = 0.14$ rad/nm for each measured time delay. The result is given by the symbols in Fig. 3. We fit this transient by an exponential function which is set to zero before $t = 0$ and convoluted by a Gaussian representing the limited time-resolution. The solid black line in Fig. 3 shows the best fit from which we extract a decay time $\tau_{\mathrm{data}} = 130 \pm 8$ ps. If we perform an analogous evaluation on the simulated data, we obtain the dashed red line. Here, the decay time is $\tau_{\mathrm{sim}} \approx 600$ ps which is essentially determined by (1) the x-ray absorption as the strain pulse propagates deeper into the substrate (absorption length at 12 keV in STO is $\approx 54\ \mu$m) and (2) normal dispersion of the phonon wavepacket. Since our lattice dynamics model does not include anharmonic phonon interactions, τ_{sim} marks an upper limit. The fact that $\tau_{\mathrm{data}} \ll \tau_{\mathrm{sim}}$ thus implies a rather efficient attenuation of the phonon wavepacket. Combining τ_{sim} and theoretical estimations including Akhiezer's mechanism of relaxation damping[17,18] and thermoelastic damping[19] yields a decay time of ≈ 200 ps which is close to our measured phonon lifetime. We also obtain very similar values (≈ 130 ps)

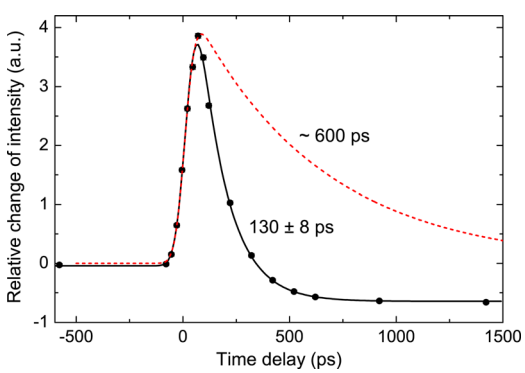

FIG. 3. (Color online) Time evolution of the integrated intensity of the 1st order sideband in Fig. 2(a) (black bullets) and the corresponding fit (solid black line). For comparison, we also show the corresponding transient obtained from the simulation which disregards anharmonic interactions in Fig. 2(b) (dashed red line).

by extrapolation of previously measured sub-GHz sound attenuation in STO (Refs. 30 and 31) according to $\tau_{\mathrm{decay}} \sim \omega^{-2}$ given by Akhiezer's damping.[17–19] More insight in the exact phonon attenuation dynamics could be gained by using shorter x-ray probe pulses since the observed phonon lifetime is close to the time-resolution of the experiment.

In conclusion, we presented UXRD data that evidence the efficient generation of quasi-monochromatic coherent LA phonon wavepackets at 140 GHz. We could explain and successfully simulate the corresponding sidebands of the STO substrate Bragg peak using a microscopic lattice dynamics model and dynamical XRD simulations. As the sidebands originate from a scattering of x-ray photons from selectively synthesized phonons with specific Q vector, the transient intensity of the sidebands directly measures the lifetime of these sub-THz LA phonons which is in accordance with theory and earlier acoustic experiments in the sub-GHz range. We believe that the combination of continuously tunable selective excitation of monochromatic phonon-pulses and UXRD will prove to be a versatile tool for investigation of sound attenuation and anharmonic phonon-phonon interactions in various materials with physically interesting coupling mechanisms at hypersonic frequencies.

We thank the BMBF for funding the project via Grant No. 05K10IP1 and the DFG via Grant No. BA2281/3-1.

[1]D. A. Reis, M. F. DeCamp, P. H. Bucksbaum, R. Clarke, E. Dufresne, M. Hertlein, R. Merlin, R. Falcone, H. Kapteyn, M. M. Murnane *et al.*, Phys. Rev. Lett. **86**, 3072 (2001).
[2]J. Larsson, A. Allen, P. H. Bucksbaum, R. W. Falcone, A. Lindenberg, G. Naylor, T. Missalla, D. A. Reis, K. Scheidt, A. Sjögren *et al.*, Appl. Phys. A **75**, 467 (2002).
[3]C. Rose-Petruck, R. Jimenez, T. Guo, A. Cavalieri, C. W. Siders, F. Rksi, J. A. Squier, B. C. Walker, K. R. Wilson, and C. P. J. Barty, Nature **398**, 310 (1999).
[4]C. Thomsen, H. T. Grahn, H. J. Maris, and J. Tauc, Phys. Rev. B **34**, 4129 (1986).
[5]E. P. N. Damen, A. F. M. Arts, and H. W. de Wijn, Phys. Rev. Lett. **74**, 4249 (1995).
[6]S. D. LeRoux, R. Colella, and R. Bray, Phys. Rev. Lett. **35**, 230 (1975).
[7]D. Roshchupkin, A. Erko, L. Ortega, and D. Irzhak, Appl. Phys. A **94**, 477 (2009).
[8]O. Synnergren, T. N. Hansen, S. Canton, H. Enquist, P. Sondhauss, A. Srivastava, and J. Larsson, Appl. Phys. Lett. **90**, 171929 (2007).
[9]J. D. Choi, T. Feurer, M. Yamaguchi, B. Paxton, and K. A. Nelson, Appl. Phys. Lett. **87**, 081907 (2005).
[10]C. Klieber, E. Peronne, K. Katayama, J. Choi, M. Yamaguchi, T. Pezeril, and K. A. Nelson, Appl. Phys. Lett. **98**, 211908 (2011).
[11]M. Bargheer, N. Zhavoronkov, Y. Gritsai, J. C. Woo, D. S. Kim, M. Woerner, and T. Elsaesser, Science **306**, 1771 (2004).
[12]P. Sondhauss, J. Larsson, M. Harbst, G. A. Naylor, A. Plech, K. Scheidt, O. Synnergren, M. Wulff, and J. S. Wark, Phys. Rev. Lett. **94**, 125509 (2005).
[13]M. Herzog, D. Schick, P. Gaal, R. Shayduk, C. v. Korff Schmising, and M. Bargheer, Appl. Phys. A **106**, 489 (2012).
[14]M. Trigo, Y. M. Sheu, D. A. Arms, J. Chen, S. Ghimire, R. S. Goldman, E. Landahl, R. Merlin, E. Peterson, M. Reason *et al.*, Phys. Rev. Lett. **101**, 025505 (2008).
[15]The sample was grown by pulsed laser deposition (Ref. 32) and included a protective coating in the form of a 1-2 nm STO capping layer.
[16]The epitaxial growth of the thin film transducer is not mandatory for generating the plane wave strain pulses. The almost perfectly matched acoustic impedances of SRO and STO ensure that there are no acoustic post-pulses and the amplitude of the strain pulses in the substrate is maximized (mass densities $\rho_{\mathrm{SRO}} = 6.26\ \mathrm{g/cm}^3$ and $\rho_{\mathrm{STO}} = 5.12\ \mathrm{g/cm}^3$, LA sound velocities $v_{\mathrm{LA}}^{\mathrm{SRO}} = 6312$ m/s and $v_{\mathrm{LA}}^{\mathrm{STO}} = 7876$ m/s from Refs. 27, 33, and 34). The impedance matching is required for the tunability of the central wavevector of the phonon wavepacket.

[17]T. O. Woodruff and H. Ehrenreich, Phys. Rev. **123**, 1553 (1961).
[18]A. Koreeda, T. Nagano, S. Ohno, and S. Saikan, Phys. Rev. B **73**, 024303 (2006).
[19]J. Y. Duquesne and B. Perrin, Phys. Rev. B **68**, 134205 (2003).
[20]M. Wulff, A. Plech, L. Eybert, R. Randler, F. Schotte, and P. Anfinrud, Faraday Discuss. **122**, 13 (2003).
[21]H. A. Navirian, M. Herzog, J. Goldshteyn, W. Leitenberger, I. Vrejoiu, D. Khakhulin, M. Wulff, R. Shayduk, P. Gaal, and M. Bargheer, J. Appl. Phys. **109**, 126104 (2011).
[22]C. von Korff Schmising, M. Bargheer, M. Kiel, N. Zhavoronkov, M. Woerner, T. Elsaesser, I. Vrejoiu, D. Hesse, and M. Alexe, Appl. Phys. B **88**, 1 (2007).
[23]C. von Korff Schmising, A. Harpoeth, N. Zhavoronkov, Z. Ansari, C. Aku-Leh, M. Woerner, T. Elsaesser, M. Bargheer, M. Schmidbauer, I. Vrejoiu *et al*., Phys. Rev. B **78**, 060404 (2008).
[24]M. Herzog, W. Leitenberger, R. Shayduk, R. van der Veen, C. J. Milne, S. L. Johnson, I. Vrejoiu, M. Alexe, and D. Hesse, Appl. Phys. Lett. **96**, 161906 (2010).
[25]C. von Korff Schmising, M. Bargheer, M. Kiel, N. Zhavoronkov, M. Woerner, T. Elsaesser, I. Vrejoiu, D. Hesse, and M. Alexe, Phys. Rev. Lett. **98**, 257601 (2007).
[26]M. Herzog, D. Schick, W. Leitenberger, R. Shayduk, R. M. van der Veen, C. J. Milne, S. L. Johnson, I. Vrejoiu, and M. Bargheer, New J. Phys. **14**, 013004 (2012).
[27]R. O. Bell and G. Rupprecht, Phys. Rev. **129**, 90 (1963).
[28]Y. H. Ren, M. Trigo, R. Merlin, V. Adyam, and Q. Li, Appl. Phys. Lett. **90**, 251918 (2007).
[29]S. A. Stepanov, E. A. Kondrashkina, R. Köhler, D. V. Novikov, G. Materlik, and S. M. Durbin, Phys. Rev. B **57**, 4829 (1998).
[30]R. Nava, R. Callarotti, H. Ceva, and A. Martinet, Phys. Lett. A **28**, 456 (1968).
[31]R. Nava, R. Callarotti, H. Ceva, and A. Martinet, Phys. Rev. **188**, 1456 (1969).
[32]I. Vrejoiu, G. Le Rhun, L. Pintilie, D. Hesse, M. Alexe, and U. Gösele, Adv. Mater. **18**, 1657 (2006).
[33]S. Yamanaka, T. Maekawa, H. Muta, T. Matsuda, S. Kobayashi, and K. Kurosaki, J. Solid State Chem. **177**, 3484 (2004).
[34]G. J. Fischer, Z. Wang, and S.-i. Karato, Phys. Chem. Miner. **20**, 97 (1993).